ASXL1 truncating mutations drive leukemic resistance to T cell attack

Dustin McCurry[1], Pavan Bachireddy[1]

[1]Department of Hematopoietic Biology and Malignancy, The University of Texas MD Anderson Cancer Center, Houston, TX, USA;

Correspondence should be sent to: pbachireddy@mdanderson.org

Summary

We previously found that specific exhausted T cell subsets defined response to donor lymphocyte infusion (DLI) in CML, a curative immunotherapy for leukemic relapse following allogeneic stem cell transplant (SCT). Since T cell states did not define resistance (GvL-r), we hypothesized that leukemic molecular pathways determine resistance. Here, we link *ASXL1* mutation status through whole exome and targeted mutation panel sequencing in two independent cohorts (78% (7/9) of non-responders and 0% (0/10) of responders) to HLA-I suppression through scRNA-seq of 138,152 myeloid cells. We identify enrichment in progenitor cell identities, notably cells enriched in the LSC17 signature in non-responders and HLA-I but not HLA-II suppression. This was confirmed in two external single cell cohorts in CMML and AML. To directly test the hypothesis that *ASXL1* mutations may suppress HLA-I, we CRISPR corrected the endogenous *ASXL1* mutation, Y591X, in K562 ($K562^m$). Wildtype reversion ($K562^c$) increased HLA-I expression at the RNA and protein level. Epigenetic profiling by CUT&RUN demonstrated increased presence of H3K4me3, but no change in H3K27me3. Prolonged treatment with EZH2i could restore HLA-I levels in $K562^m$ cells. $K562^c$ and $K562^m$ were also used to prime antigen specific T-cells to test T-cell cytotoxicity. Primed T-cells preferentially killed $K562^c$ vs $K562^m$ without and with IFNγ pre-treatment, though EZH2i rendered $K562^m$ equally susceptible to T cell killing as $K562^c$. In summary, we integrated molecular analyses with immuno-functional studies to define a novel oncogenetic pathway of immune evasion. Specifically, we link GvL-r to $ASXL1^m$ that suppresses transcription of HLA-I and antigen presentation machinery in myeloid diseases; moreover, its correction restores anti-leukemic CD8+ T-cell cytotoxicity.

Main Text

The therapeutic graft-versus-leukemia (GvL) effect is critical to the clinical activity of allogeneic stem cell transplantation (allo-SCT), a potentially curative form of immunotherapy for patients with leukemia.[1–3] GvL resistance (GvL-r) is a critical driver of morbidity and mortality following allo-SCT as outcomes following leukemic relapse are dismal.[3] One approach that seeks to address GvLr is donor lymphocyte infusion (DLI),[3–6] an adoptive immunotherapy with a spectrum of clinical activity. To probe the drivers of GvL-r in response to DLI, we previously characterized the T cell states in responders (R) or non-responders (NR).[7] Strikingly, we identified that specific exhausted T cell subsets defined DLI responders (DLI-R); though we were unable to identify a pattern of T cell dysfunction in non-responders (DLI-NR)[7] suggesting

that some forms of GvL-r may be mediated by T cell extrinsic features. Thus, we hypothesized that leukemic molecular features may define resistance to DLI, informing our understanding of GvL-r.

To test this hypothesis, we assembled a cohort of 14 patients treated with CD8-depleted DLI for relapsed CML following allo-SCT. Eight patients were long-term DLI-R, defined as having achieved molecular remission (i.e., RT-PCR negative for the BCR-ABL transcript) after DLI, and six were DLI-NR, who did not achieve molecular remission following DLI. As published previously, none of the patients developed acute graft-versus-host disease (GvHD) after DLI and the timing between allo-SCT and DLI therapy was comparable between DLI-R and DLI-NR.[7] As a reference, we also analyzed post-transplant BM biopsies from two patients with CML who never relapsed after allo-SCT, and as a confirmation cohort, we assembled an independent set of six patients (1 R and 5 NR) treated with CD8-depleted DLI for relapsed CML at a separate institution. In this independent cohort, one patient developed GvHD following DLI. Serial BM or PB samples were collected at a median of 3 time points per patient. Whole exome sequencing was performed on 49 samples from 11 patients within the discovery cohort. A targeted mutation panel[8] was performed on seven samples from the independent cohort of six patients. For 46 samples, we obtained single-cell RNA sequencing (scRNA-seq) data on viable mononuclear cells. Additional cohorts consisted of single-cell chromatin accessibility sequencing (scATAC-seq) in five patients with chronic monomyelocytic leukemia (CMML)[9] and nine patients with acute myeloid leukemia (AML)[10] (**Figure 1a**).

<u>Identification of *ASXL1* mutations in DLI resistance</u>

Within the discovery cohort we obtained genomic DNA from recipient-derived mesenchymal stromal cells (R-MSC) and donor peripheral blood cells (D-PBC) for germline sources in eleven patients (7 R and 4 NR). To identify somatic alterations, we used MuTect2 with R-MSC and D-PBC as controls. Given the prognostic role of additional oncogenic driver mutations in CML, both in the pre- and post-TKI era,[11] we sought to identify mutations in known leukemic driver genes. Strikingly, no recurrent mutations in known cancer drivers were identified at post-SCT relapse time points in patients that responded to DLI. We identified recurrent mutations in *ASXL1*, *IKZF1*, and *RUNX1* in 14 of 44 samples (31.82%), all from patients that did not respond to DLI (NR) (**Figure 1b**). Known non-Philadelphia (Ph) chromosome cancer drivers were found in 4/4 DLI-NRs (*RUNX1* (1/4), *IKZF1* (2/4), and truncating exon 12 *ASXL1* mutations (*ASXL1*^{m}) (3/4)). *ASXL1*, IKZF1, and RUNX1 mutations are linked to prognosis, advanced-phase, and myeloid and/or lymphoid skewing in CML.[11] All IKZF1 mutations (2/4) were predominantly missense mutations, in contrast to nonsense or frameshift mutations more commonly reported in CML.[12] Each patient with an IKZF1 mutation had a concurrent *ASXL1*^{m}, and one additional DLI-NR was found to have an *ASXL1*^{m} only. One patient had a frame-shift mutation in RUNX1, a common mutation type in myeloid malignancies.[13] All *ASXL1* mutations identified in 3/4 NR were frameshift or nonsense mutations within exon 12 prior to the plant homeodomain (PHD), consistent with the commonly mutated region in myeloid malignancies.[14–16] These mutations are reported to produce a truncated protein with altered function. We sought to determine whether these findings were reproducible, so we performed targeted mutation sequencing[8] on seven samples from an independent cohort of six CML patients (1 R and 5 NR) treated with

CD8-depleted DLI at MD Anderson Cancer Center. We identified *ASXL1* mutations in 4/5 NR and 0/1 R. The most common mutation was E635fs (2 patients) (**Figure 1c**). In total, we identified *ASXL1* exon 12 nonsense or frame-shift mutations in 7/9 NR (78%) and 0/8 R (0%) (p=7e-4, two-sided Fisher's test) (**Figure 1d**). In one patient, 5318, DLI heralded the emergence of mutant *ASXL1*, further rising over time, suggesting clonal evolution of the CML following DLI, despite the same Ph-chromosome positivity at all time points (**Figure 1e**).

Given the potential role for neoantigens to participate in the GvL response, we also calculated the tumor mutation burden (TMB),[17,18] and sought to determine determine whether DLI response is associated with TMB or predicted neoantigens with strong binding affinity (defined as binding affinity ≤50 nM by netMHCpan). Our prior findings[17,18] suggested that neoantigen specific responses are maintained in long-term responders to allo-SCT and depleted in patients who relapse late after allo-SCT. We did not identify either TMB or predicted high affinity neoantigen burden as predictive biomarkers for DLI response (**Figure 1f)**. Two patients received greater than one allo-SCT prior to DLI, limiting the ability to calculate a total mutational burden for these patients.

Identification of leukemic cells in scRNA-seq Data

The emergence of *ASXL1* mutations in NR led us to hypothesise that DLI resistance may be mediated by leukemic intrinsic features shaped by *ASXL1* mutations. To test this hypothesis, we interrogated our cohort of scRNA-seq samples. In total, this cohort was composed of 57 samples from 17 patients (8 R, 6 NR, and 2 patients who never relapsed). Following batch correction (Harmony) and quality filtering, we identified 388,952 cells passing QC (**Figure 2a**). Consistent with findings in other chronic myeloid malignancies,[20] we identified intact hematopoietic lineages, including T-cells, B-cells, megakaryocyte-erythroid precursors (MEP), and monocytes (Figure 2a). To identify leukemic cells, we integrated our WES sequencing to identify expression of mutant transcripts (**Figure 2b**). Mutant cells were largely confined to the myeloid compartment. Mutant cells composed 0.19% of all cells, which was correlated with Ph+ burden (**Figure 2b**). Consistent with the known challenges of detecting *ASXL1* mutations in scRNA-seq data, we were unable to detect *ASXL1* mutant cells.[21,22]

Given the low frequency of mutant cells when integrating WES with scRNA-seq data, we attempted other approaches to identify leukemic cells to assess leukemic intrinsic features. A machine learning approach based upon transcriptional states of known mutant cells from exome data[23] (**Figure 2c**) demonstrated over a ten-fold increase in mutant cell yield (9.1%), but was not well correlated with Ph+ burden (**Figure 2c**). In a subset of cases, alloSCT were performed with sex mismatched donors, enabling detection of Y-chromosome derived transcripts uniquely in the donor or recipient, enabling calculation of a donor-recipient score (D/R score). This measure was correlated with Ph+ burden, and identified 37.5% of mutant cells (**Figure 2d**).

DLI-r links to suppressed HLA-I in LSC Compartment

Given the predominance of recipient cells within the myeloid compartment, we performed a reclustering of the myeloid compartment in Scanpy with a force directed layout[24] to better assess the relationships between cell states (**Figure 2e**). To identify hematopoietic trajectories

and transitions in cell state, Monocle 3 was used[25] (**Figure 2f**). We identified a progenitor cell state and were able to recapitulate known hematopoietic differentiation trajectories, including erythroid, myeloid, and megakaryocytic lineages. Gene programs identified in differentiating hematopoietic progenitors identified in post stem-cell transplant bone marrow samples were used.[26] Within this re-clustering, we continued to identify intact hematopoietic lineages consistent with our prior finding (**Figure 2e,2f**). To assess for cellular states that herald DLI resistance, we performed a differential enrichment analysis based on responders or nonresponders at timepoints immediately prior to DLI. This identified one cluster composed of monocytes enriched in R (**Figure 3a**), consistent with results in other cancer types treated with PD-1 immunotherapy.[27] In nonresponders, we identified four progenitor clusters enriched in non-responders composed of granulocyte-monocyte progenitors (GMP), basophil and eosinophil progenitors (Eo/BPro), megakaryocyte progenitors (MkP), and a hematopoietic stem cell-like cluster (HSC).

We next sought to determine if these clusters were enriched in recipient cells utilising our D/R-score. This demonstrated that multiple clusters were enriched in recipient cells (**Figure 3b**). The four clusters enriched in non-responders were composed of varying proportions of recipient cells, with the composition of the GMP cluster being distributed across donor and recipient cells. In contrast, the HSC-like cluster was enriched in recipient cells, consistent with the known existence of BCR-ABL mutant CD34+ progenitors in CML.[28,29]

Given that CD34+ BCR-ABL mutant CD34+ progenitors are known to be a source of CML leukemic stem cells (LSC) [11,28–32] we sought to further characterize this HSC-like cluster. Using multiple transcriptional signatures for LSC (**Figure 3c**), we identified that this cluster demonstrated transcriptional evidence of being bona-fide LSC. Next, we sought to investigate potential immune escape mechanisms within this cluster. Given the known role for HLA dysregulation at leukemic relapse following alloSCT[33–37] we examined HLA-I and HLA-II gene expression. Surprisingly, we did not identify alterations in HLA-II expression [33,36,37] (**Figure 3d**). In contrast we identified decreased HLA-I (HLA-A,B,C) expression in DLI-NR that was maintained when also accounting for B2M (**Figure 3e**). These findings suggested that *ASXL1*-mutations may mediate immune escape through suppression of HLA-I expression.

<u>Validation in additional *ASXL1* mutant cohorts</u>

To test this hypothesis in additional myeloid malignancies, we probed existing datasets in *ASXL1* mutant myeloid malignancies. A data set of nine patients with acute myeloid leukemia (AML)[10] demonstrated that in a cluster with enrichment in LSC-signatures, cells from patients with *ASXL1*-mutant leukemia demonstrated significantly decreased HLA-I (HLA-A,B,B2M) (**Figure 3f**). Separately in a cohort comprised of five patients with chronic monomyelocytic leukemia (CMML)[9], we utilised single-cell chromatin accessibility sequencing (scATAC-seq) data to identify clusters with higher accessibility of LSC-related genes and evaluated the accessibility of HLA-I genes. Consistent with the lower dynamic range of scATAC-seq[38], there was decreased accessibility of HLA-I (HLA-A,B,C,B2M) in *ASXL1*-mutant cases, though this difference was less than in the scAML cohort (**Figure 3g**).

Functional interrogation in leukemic cell lines

To functionally interrogate the contribution of *ASXL1* mutations to HLA-I suppression, we characterized K562, a pluripotent hematopoietic stem cell like cell line derived from a CML patient in blast crisis carrying an *ASXL1* mutation (Y591X)[39–44] known to be HLA-I negative. Utilizing CRISPR-Cas9 we corrected the *ASXL1* Y591X mutation ($K562^m$)[45] (**Figure 4a**) resulting in isogenic K562 cell lines differing in the presence of the *ASXL1* mutation. To test for HLA-expression, cell surface flow cytometry demonstrated significantly increased HLA-I but not HLA-II (**Figure 4b, 4c**) following *ASXL1* Y591 correction ($K562^c$). Treatment with interferon-gamma (IFNγ) is known to potently increase cell surface HLA-I in K562,[46] so we treated both cell lines with IFNγ. The $K562^c$ cell line demonstrated significantly increased HLA-I compared to $K562^m$ (**Figure 4a,4b**), though neither were able to increase HLA-II. To determine whether changes in HLA-I were due to increased transcription, we performed RNA-seq of the isogenic cell lines. $K562^c$ demonstrated significantly increased HLA-I expression (**Figure 4d**).

Since *ASXL1* is a known chromatin remodeler, we hypothesized that the changes in transcription may be driven by epigenetic alterations. We profiled H3K4me3 and H3K27me3, as the presence of these marks at the same histone results in a state of bivalency that results in tightly regulated gene transcription. Moreover, *ASXL1* mutations have been implicated in altered H3K4me3 distribution across the genome. At both HLA-B and HLA-C, we did not detect alterations in H3K27me3, but did identify differentially enriched peaks at both HLA-B and HLA-C (**Figure 4e**).

H3K27me3 is deposited by the Polycomb Repressive Complex 2 (PRC2) through the enzymatically functional subunit, Enhancer of Zeste 2 (EZH2). Inhibitors of EZH2 (EZH2i) are being tested in multiple malignancies and are approved in follicular lymphoma. Given our finding of preserved H3K27me3 at HLA-genes in the isogenic cell lines, we hypothesized that treatment with EHZ2i would increase HLA in both cell lines. Consistent with this, we identified that treatment with EZH2i over 5 days can increase cell surface HLA in both $K562^m$ and $K562^c$ cell lines, with $K562^c$ cell line achieving nearly university HLA-I positivity (**Figure 4f**). Following an extended treatment with EZH2i over nine days, both cell lines achieved nearly universal HLA-I expression (**Figure 4g**).

ASXL1 correction restores T-cell attack

We next sought to determine whether correcting $ASXL1^m$ could restore T-cell targeting of K562 by T-cells. To do this, we developed a K562 T-cell recognition assay built upon our prior work generating antigen-specific T-cells[47] (**Figure 5a**). Replacing peptide antigen with a 50%/50% mixture of irradiated IFNγ pre-treated $K562^m$ and $K562^c$ isogenic cell lines, we expanded T-cells with IL-7 (40ng/mL) and IL-2 (150IU) over the course of 14 days, before restimulating T-cells with a fresh 50%/50% mixture of irradiated IFNγ pre-treated $K562^m$ and $K562^c$ isogenic cell lines. After 21 days of total culture, T-cells were co-cultured with CellTrace™ Violet (CTV) labeled $K562^m$ and $K562^c$ over 18 hours before staining with viability dye and cell surface markers. Control T-cells were stimulated with anti-CD3 and anti-CD28 beads for 1 week prior to co-culture. K562 primed T-cells demonstrated preferential recognition of $K562^c$ compared to control T-cells, while $K562^m$ demonstrated no preferential recognition even at 10:1 E:T ratio

(**Figure 5b**). Co-staining of CD3, CD8, and CD137 demonstrated upregulation of CD137 in K562 primed T-cells upon $K562^c$ co-culture and not $K562^m$ (**Figure 5c**).

We then pretreated $K562^m$ and $K562^c$ with either IFNγ (24 hours) or EZH2i (5 days) prior to CTV labeling to determine whether these agents could enhance T-cell killing of $K562^c$ and $K562^m$. Pretreatment with IFNγ enhanced T-cell recognition of $K562^c$ and enabled preferential T cell killing of $K562^m$ compared to control T-cells, though primed T-cells killed $K562^c$ much more readily than $K562^m$ (**Figure 5d**). In contrast, pre-treatment with EZH2i enabled T-cell killing of $K562^c$ and $K562^m$ at similar levels, suggesting that EZH2i may be able to circumvent $ASXL1^m$ suppression of T-cell recognition and killing (**Figure 5e**).

Taken altogether, our findings identify a new oncogenetic pathway that governs the expression of HLA-I in myeloid malignancies. Additionally, we define how ASXL1 mutations shape epigenetic marks that regulate transcription of HLA-genes. Moreover, we identify EZH2i as a potential agent, in contrast to IFNγ that can overcome ASXL1 mediated HLA-I suppression. Finally, correcting ASXL1 mutations or treatment with EZH2i can enable T cell killing of ASXL1 mutant leukemia.

Methods

Human subjects

Bone marrow (BM) biopsies were obtained pre- and post-DLI after relapse following alloSCT (or during remission following alloSCT) from patients enrolled in Dana-Farber Cancer Institute (DFCI) clinical trials (94-009, 95-011, 96-372, 96-022, and 96-277) between 1994-2001 that were approved by the DFCI Human Subjects Protection Committee. These studies were conducted in accordance with the Declaration of Helsinki; informed consent was obtained from the patients. Bone marrow mononuclear cells (BMMCs) were isolated via Ficoll-Hypaque density gradient centrifugation, cryopreserved with 10% dimethyl sulfoxide, and stored in vapor-phase liquid nitrogen until the time of sample processing.

Cohort sample characteristics

All 17 patients had CML that was treated with CD8 T cell depleted alloSCT. Of these, 15 patients had CML relapse after alloSCT that was treated with CD8-depleted DLI, and 2 patients never had CML relapse and served as non-relapse controls. DLIs were infused at weekly intervals until the target cell dose was reached.

Sample processing

Cryopreserved primary bone marrow mononuclear cells (BMMCs) were thawed on the day of sequencing at 37C and dispensed drop-wise into a warmed solution of 10% FBS, 10% DNaseI (StemCell Technologies, cat. No. 07900) in PBS. The cell suspension was centrifuged at 200 g for 10 minutes at room temperature. Viable cells were negatively selected using MACS Dead Cell Removal Kit (Miltenyi Biotec, cat. No. 130-090-101), running on MS columns to prevent sample loss. Collected live cells were resuspended in 0.04% BSA in PBS and diluted to a

concentration of 1000 cells/uL. These cells were then divided into portions taken immediately for scRNA-seq.

References

1. Bachireddy, P., Burkhardt, U.E., Rajasagi, M., and Wu, C.J. (2015). Haematological malignancies: at the forefront of immunotherapeutic innovation. Nat Rev Cancer *15*, 201–215. https://doi.org/10.1038/nrc3907.

2. Socie, G., Zeiser, R., and Blazar, B.R. (2018). Immune Biology of Allogeneic Hematopoietic Stem Cell Transplantation: Models in Discovery and Translation (Academic Press).

3. Jenq, R.R., and van den Brink, M.R.M. (2010). Allogeneic haematopoietic stem cell transplantation: individualized stem cell and immune therapy of cancer. Nat Rev Cancer *10*, 213–221. https://doi.org/10.1038/nrc2804.

4. Bachireddy, P., and Wu, C.J. (2014). Understanding anti-leukemia responses to donor lymphocyte infusion. Oncoimmunology *3*, e28187. https://doi.org/10.4161/onci.28187.

5. Bachireddy, P., Hainz, U., Rooney, M., Pozdnyakova, O., Aldridge, J., Zhang, W., Liao, X., Hodi, F.S., O'Connell, K., Haining, W.N., et al. (2014). Reversal of in situ T-cell exhaustion during effective human antileukemia responses to donor lymphocyte infusion. Blood *123*, 1412–1421. https://doi.org/10.1182/blood-2013-08-523001.

6. Schmid, C., Kuball, J., and Bug, G. (2021). Defining the Role of Donor Lymphocyte Infusion in High-Risk Hematologic Malignancies. J Clin Oncol *39*, 397–418. https://doi.org/10.1200/JCO.20.01719.

7. Bachireddy, P., Azizi, E., Burdziak, C., Nguyen, V.N., Ennis, C.S., Maurer, K., Park, C.Y., Choo, Z.-N., Li, S., Gohil, S.H., et al. (2021). Mapping the evolution of T cell states during response and resistance to adoptive cellular therapy. Cell Rep *37*, 109992. https://doi.org/10.1016/j.celrep.2021.109992.

8. Chen, K., Meric-Bernstam, F., Zhao, H., Zhang, Q., Ezzeddine, N., Tang, L.-Y., Qi, Y., Mao, Y., Chen, T., Chong, Z., et al. (2015). Clinical actionability enhanced through deep targeted sequencing of solid tumors. Clin Chem *61*, 544–553. https://doi.org/10.1373/clinchem.2014.231100.

9. Binder, M., Carr, R.M., Lasho, T.L., Finke, C.M., Mangaonkar, A.A., Pin, C.L., Berger, K.R., Mazzone, A., Potluri, S., Ordog, T., et al. (2022). Oncogenic gene expression and epigenetic remodeling of cis-regulatory elements in ASXL1-mutant chronic myelomonocytic leukemia. Nat Commun *13*, 1434. https://doi.org/10.1038/s41467-022-29142-6.

10. Dufva, O., Pölönen, P., Brück, O., Keränen, M.A.I., Klievink, J., Mehtonen, J., Huuhtanen, J., Kumar, A., Malani, D., Siitonen, S., et al. (2020). Immunogenomic Landscape of Hematological Malignancies. Cancer Cell *38*, 424–428. https://doi.org/10.1016/j.ccell.2020.08.019.

11. Bidikian, A., Kantarjian, H., Jabbour, E., Short, N.J., Patel, K., Ravandi, F., Sasaki, K., and Issa, G.C. (2022). Prognostic impact of ASXL1 mutations in chronic phase chronic myeloid

leukemia. Blood Cancer Journal *12*, 144. https://doi.org/10.1038/s41408-022-00742-1.

12. Feng, L., Zhang, H., and Liu, T. (2024). Multifaceted roles of gene, perspectives from bench to bedside. Front Oncol *14*, 1383419. https://doi.org/10.3389/fonc.2024.1383419.

13. Jayne, N.D., Liang, Z., Lim, D.-H., Chen, P.B., Diaz, C., Arimoto, K.-I., Xia, L., Liu, M., Ren, B., Fu, X.-D., et al. (2024). RUNX1 C-terminal mutations impair blood cell differentiation by perturbing specific enhancer-promoter networks. Blood Adv *8*, 2410–2423. https://doi.org/10.1182/bloodadvances.2023011484.

14. Gao, X., You, X., Droin, N., Banaszak, L.G., Churpek, J., Padron, E., Geissler, K., Solary, E., Patnaik, M.M., and Zhang, J. (2022). Role of ASXL1 in hematopoiesis and myeloid diseases. Exp Hematol *115*, 14–19. https://doi.org/10.1016/j.exphem.2022.09.003.

15. Medina, E.A., Delma, C.R., and Yang, F.-C. (2022). ASXL1/2 mutations and myeloid malignancies. J Hematol Oncol *15*, 127. https://doi.org/10.1186/s13045-022-01336-x.

16. Johnson, S.M., Haberberger, J., Galeotti, J., Ramkissoon, L., Coombs, C.C., Richardson, D.R., Foster, M.C., Duncan, D., Zeidner, J.F., Ferguson, N.L., et al. (2023). A reappraisal of ASXL1 mutation sites and the cohesin-binding motif in myeloid disease. Blood Cancer J *13*, 96. https://doi.org/10.1038/s41408-023-00876-w.

17. Bachireddy, P., Ennis, C., Nguyen, V.N., Gohil, S.H., Clement, K., Shukla, S.A., Forman, J., Barkas, N., Freeman, S., Bavli, N., et al. (2020). Distinct evolutionary paths in chronic lymphocytic leukemia during resistance to the graft-versus-leukemia effect. Sci Transl Med *12*. https://doi.org/10.1126/scitranslmed.abb7661.

18. Rajasagi, M., Shukla, S.A., Fritsch, E.F., Keskin, D.B., DeLuca, D., Carmona, E., Zhang, W., Sougnez, C., Cibulskis, K., Sidney, J., et al. (2014). Systematic identification of personal tumor-specific neoantigens in chronic lymphocytic leukemia. Blood *124*, 453–462. https://doi.org/10.1182/blood-2014-04-567933.

19. Alexandrov, L.B., Kim, J., Haradhvala, N.J., Huang, M.N., Tian Ng, A.W., Wu, Y., Boot, A., Covington, K.R., Gordenin, D.A., Bergstrom, E.N., et al. (2020). The repertoire of mutational signatures in human cancer. Nature *578*, 94–101. https://doi.org/10.1038/s41586-020-1943-3.

20. Nam, A.S., Kim, K.-T., Chaligne, R., Izzo, F., Ang, C., Taylor, J., Myers, R.M., Abu-Zeinah, G., Brand, R., Omans, N.D., et al. (2019). Somatic mutations and cell identity linked by Genotyping of Transcriptomes. Nature *571*, 355–360. https://doi.org/10.1038/s41586-019-1367-0.

21. Griffin, G.K., Booth, C.A.G., Togami, K., Chung, S.S., Ssozi, D., Verga, J.A., Bouyssou, J.M., Lee, Y.S., Shanmugam, V., Hornick, J.L., et al. (2023). Ultraviolet radiation shapes dendritic cell leukaemia transformation in the skin. Nature *618*, 834–841. https://doi.org/10.1038/s41586-023-06156-8.

22. Ediriwickrema, A., Gentles, A.J., and Majeti, R. (2023). Single-cell genomics in AML: extending the frontiers of AML research. Blood *141*, 345–355. https://doi.org/10.1182/blood.2021014670.

23. van Galen, P., Hovestadt, V., Wadsworth, M.H., Ii, Hughes, T.K., Griffin, G.K., Battaglia, S.,

Verga, J.A., Stephansky, J., Pastika, T.J., Lombardi Story, J., et al. (2019). Single-Cell RNA-Seq Reveals AML Hierarchies Relevant to Disease Progression and Immunity. Cell *176*, 1265–1281.e24. https://doi.org/10.1016/j.cell.2019.01.031.

24. Weinreb, C., Wolock, S., and Klein, A.M. (2018). SPRING: a kinetic interface for visualizing high dimensional single-cell expression data. Bioinformatics *34*, 1246–1248. https://doi.org/10.1093/bioinformatics/btx792.

25. Trapnell, C., Cacchiarelli, D., Grimsby, J., Pokharel, P., Li, S., Morse, M., Lennon, N.J., Livak, K.J., Mikkelsen, T.S., and Rinn, J.L. (2014). The dynamics and regulators of cell fate decisions are revealed by pseudotemporal ordering of single cells. Nat Biotechnol *32*, 381–386. https://doi.org/10.1038/nbt.2859.

26. Huo, Y., Wu, L., Pang, A., Li, Q., Hong, F., Zhu, C., Yang, Z., Dai, W., Zheng, Y., Meng, Q., et al. (2023). Single-cell dissection of human hematopoietic reconstitution after allogeneic hematopoietic stem cell transplantation. Sci Immunol *8*, eabn6429. https://doi.org/10.1126/sciimmunol.abn6429.

27. Krieg, C., Nowicka, M., Guglietta, S., Schindler, S., Hartmann, F.J., Weber, L.M., Dummer, R., Robinson, M.D., Levesque, M.P., and Becher, B. (2018). High-dimensional single-cell analysis predicts response to anti-PD-1 immunotherapy. Nat Med *24*, 144–153. https://doi.org/10.1038/nm.4466.

28. Chu, S., Xu, H., Shah, N.P., Snyder, D.S., Forman, S.J., Sawyers, C.L., and Bhatia, R. (2005). Detection of BCR-ABL kinase mutations in CD34+ cells from chronic myelogenous leukemia patients in complete cytogenetic remission on imatinib mesylate treatment. Blood *105*, 2093–2098. https://doi.org/10.1182/blood-2004-03-1114.

29. Bhatia, R., Holtz, M., Niu, N., Gray, R., Snyder, D.S., Sawyers, C.L., Arber, D.A., Slovak, M.L., and Forman, S.J. (2003). Persistence of malignant hematopoietic progenitors in chronic myelogenous leukemia patients in complete cytogenetic remission following imatinib mesylate treatment. Blood *101*, 4701–4707. https://doi.org/10.1182/blood-2002-09-2780.

30. Warfvinge, R., Geironson, L., Sommarin, M.N.E., Lang, S., Karlsson, C., Roschupkina, T., Stenke, L., Stentoft, J., Olsson-Strömberg, U., Hjorth-Hansen, H., et al. (2017). Single-cell molecular analysis defines therapy response and immunophenotype of stem cell subpopulations in CML. Blood *129*, 2384–2394. https://doi.org/10.1182/blood-2016-07-728873.

31. Giustacchini, A., Thongjuea, S., Barkas, N., Woll, P.S., Povinelli, B.J., Booth, C.A.G., Sopp, P., Norfo, R., Rodriguez-Meira, A., Ashley, N., et al. (2017). Single-cell transcriptomics uncovers distinct molecular signatures of stem cells in chronic myeloid leukemia. Nat Med *23*, 692–702. https://doi.org/10.1038/nm.4336.

32. Krishnan, V., Schmidt, F., Nawaz, Z., Venkatesh, P.N., Lee, K.L., Ren, X., Chan, Z.E., Yu, M., Makheja, M., Rayan, N.A., et al. (2023). A single-cell atlas identifies pretreatment features of primary imatinib resistance in chronic myeloid leukemia. Blood *141*, 2738–2755. https://doi.org/10.1182/blood.2022017295.

33. Toffalori, C., Zito, L., Gambacorta, V., Riba, M., Oliveira, G., Bucci, G., Barcella, M., Spinelli, O., Greco, R., Crucitti, L., et al. (2019). Immune signature drives leukemia escape and

relapse after hematopoietic cell transplantation. Nat Med *25*, 603–611. https://doi.org/10.1038/s41591-019-0400-z.

34. Han, X., Zhao, J., Liu, J., Guo, D., Li, H., and Fan, S. (2022). Loss of mismatched HLA in acute myeloid leukemia relapse after haploidentical peripheral blood stem cell transplantation combined with unrelated cord blood: A case report. Transpl Immunol *73*, 101602. https://doi.org/10.1016/j.trim.2022.101602.

35. Rovatti, P.E., Gambacorta, V., Lorentino, F., Ciceri, F., and Vago, L. (2020). Mechanisms of Leukemia Immune Evasion and Their Role in Relapse After Haploidentical Hematopoietic Cell Transplantation. Front Immunol *11*, 147. https://doi.org/10.3389/fimmu.2020.00147.

36. Gambacorta, V., Beretta, S., Ciccimarra, M., Zito, L., Giannetti, K., Andrisani, A., Gnani, D., Zanotti, L., Oliveira, G., Carrabba, M.G., et al. (2022). Integrated Multiomic Profiling Identifies the Epigenetic Regulator PRC2 as a Therapeutic Target to Counteract Leukemia Immune Escape and Relapse. Cancer Discov *12*, 1449–1461. https://doi.org/10.1158/2159-8290.CD-21-0980.

37. Christopher, M.J., Petti, A.A., Rettig, M.P., Miller, C.A., Chendamarai, E., Duncavage, E.J., Klco, J.M., Helton, N.M., O'Laughlin, M., Fronick, C.C., et al. (2018). Immune Escape of Relapsed AML Cells after Allogeneic Transplantation. N Engl J Med *379*, 2330–2341. https://doi.org/10.1056/NEJMoa1808777.

38. Yan, F., Powell, D.R., Curtis, D.J., and Wong, N.C. (2020). From reads to insight: a hitchhiker's guide to ATAC-seq data analysis. Genome Biol *21*, 22. https://doi.org/10.1186/s13059-020-1929-3.

39. Lozzio, B.B., Lozzio, C.B., Bamberger, E.G., and Feliu, A.S. (1981). A multipotential leukemia cell line (K-562) of human origin. Proc Soc Exp Biol Med *166*, 546–550. https://doi.org/10.3181/00379727-166-41106.

40. Lozzio, C.B., and Lozzio, B.B. (1975). Human chronic myelogenous leukemia cell-line with positive Philadelphia chromosome. Blood *45*, 321–334.

41. Andersson, L.C., Nilsson, K., and Gahmberg, C.G. (1979). K562--a human erythroleukemic cell line. Int J Cancer *23*, 143–147. https://doi.org/10.1002/ijc.2910230202.

42. Andersson, L.C., Jokinen, M., and Gahmberg, C.G. (1979). Induction of erythroid differentiation in the human leukaemia cell line K562. Nature *278*, 364–365. https://doi.org/10.1038/278364a0.

43. Ge, G., Zhang, P., Sui, P., Chen, S., Yang, H., Guo, Y., Rubalcava, I.P., Noor, A., Delma, C.R., Agosto-Peña, J., et al. (2024). Targeting lysine demethylase 6B ameliorates ASXL1 truncation-mediated myeloid malignancies in preclinical models. J Clin Invest *134*. https://doi.org/10.1172/JCI163964.

44. Garson, D., Dokhélar, M.C., Wakasugi, H., Mishal, Z., and Tursz, T. (1985). HLA class-I and class-II antigen expression by human leukemic K562 cells and by Burkitt-K562 hybrids: modulation by differentiation inducers and interferon. Exp Hematol *13*, 885–890.

45. Köhnke, T., Nuno, K.A., Alder, C.C., Gars, E.J., Phan, P., Fan, A.C., and Majeti, R. (2024). Human ASXL1-Mutant Hematopoiesis Is Driven by a Truncated Protein Associated with

Aberrant Deubiquitination of H2AK119. Blood Cancer Discov *5*, 202–223. https://doi.org/10.1158/2643-3230.BCD-23-0235.

46. Maziarz, R.T., Mentzer, S.J., Burakoff, S.J., and Faller, D.V. (1990). Distinct effects of interferon-gamma and MHC class I surface antigen levels on resistance of the K562 tumor cell line to natural killer-mediated lysis. Cell Immunol *130*, 329–338. https://doi.org/10.1016/0008-8749(90)90276-w.

47. Pathangey, L.B., McCurry, D.B., Gendler, S.J., Dominguez, A.L., Gorman, J.E., Pathangey, G., Mihalik, L.A., Dang, Y., Disis, M.L., and Cohen, P.A. (2017). Surrogate in vitro activation of innate immunity synergizes with interleukin-7 to unleash rapid antigen-driven outgrowth of CD4+ and CD8+ human peripheral blood T-cells naturally recognizing MUC1, HER2/neu and other tumor-associated antigens. Oncotarget *8*, 10785–10808. https://doi.org/10.18632/oncotarget.13911.

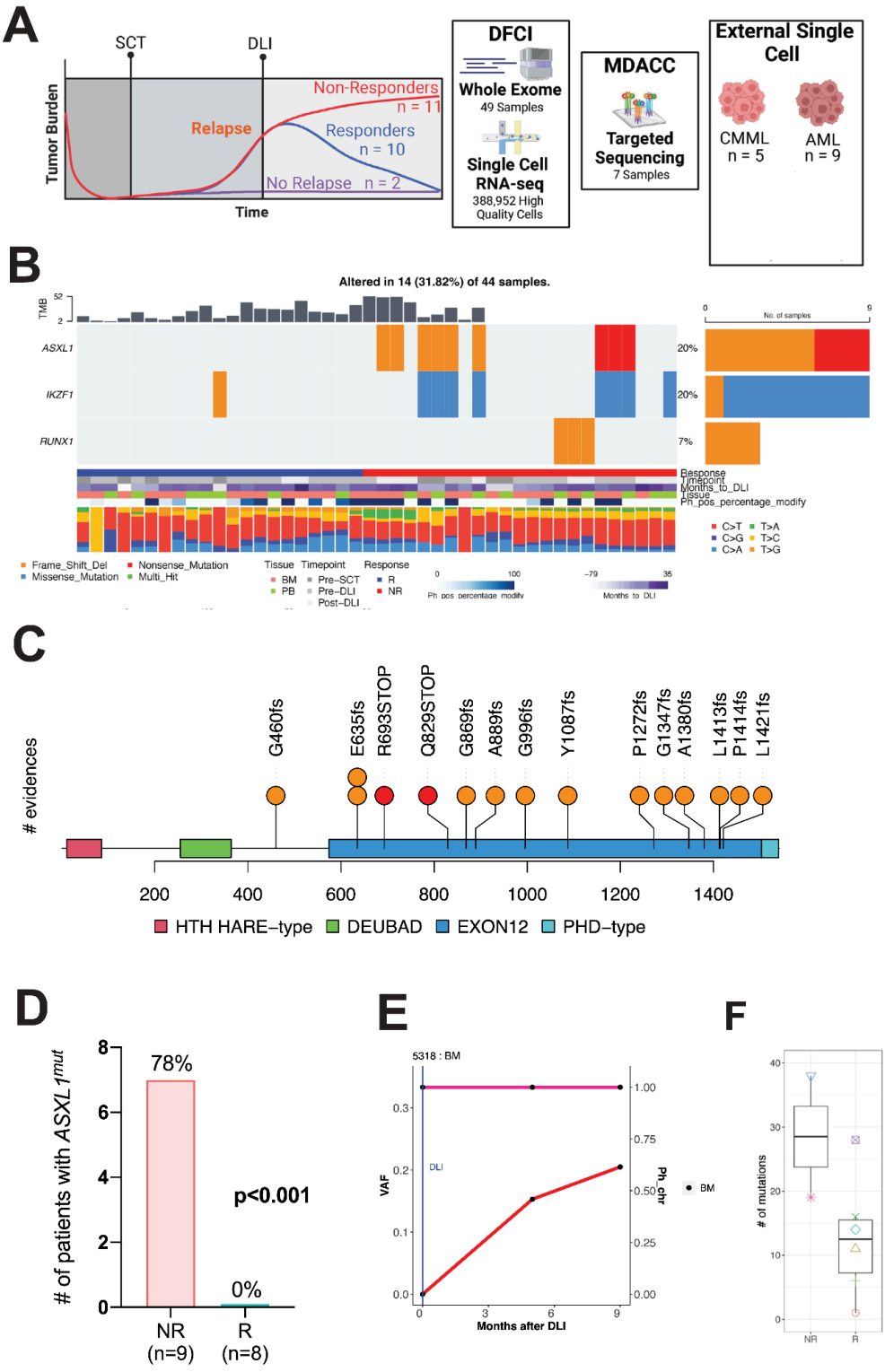
A
SCT
DLI
Tumor Burden
Relapse
Non-Responders
n = 11
Responders
n = 10
No Relapse n = 2
Time
DFCI
Whole Exome
49 Samples
Single Cell
RNA-seq
388,952 High
Quality Cells
MDACC
Targeted
Sequencing
7 Samples
External Single
Cell
CMML
n = 5
AML
n = 9
B
Altered in 14 (31.82%) of 44 samples.
TMB
ASXL1
IKZF1
RUNX1
20%
20%
7%
No. of samples
Response
Timepoint
Months_to_DLI
Tissue
Ph_pos_percentage_modify
C>T
C>G
C>A
T>A
T>C
T>G
Frame_Shift_Del
Missense_Mutation
Nonsense_Mutation
Multi_Hit
Tissue
BM
PB
Timepoint
Pre-SCT
Pre-DLI
Post-DLI
Response
R
NR
Ph_pos_percentage_modify
Months_to_DLI
C
evidences
G460fs
E635fs
R693STOP
Q829STOP
G869fs
A889fs
G996fs
Y1087fs
P1272fs
G1347fs
A1380fs
L1413fs
P1414fs
L1421fs
200
400
600
800
1000
1200
1400
HTH HARE-type
DEUBAD
EXON12
PHD-type
D
# of patients with ASXL1mut
78%
0%
p<0.001
NR
(n=9)
R
(n=8)
E
5318 : BM
VAF
Ph chr
DLI
BM
Months after DLI
F
# of mutations
NR
R

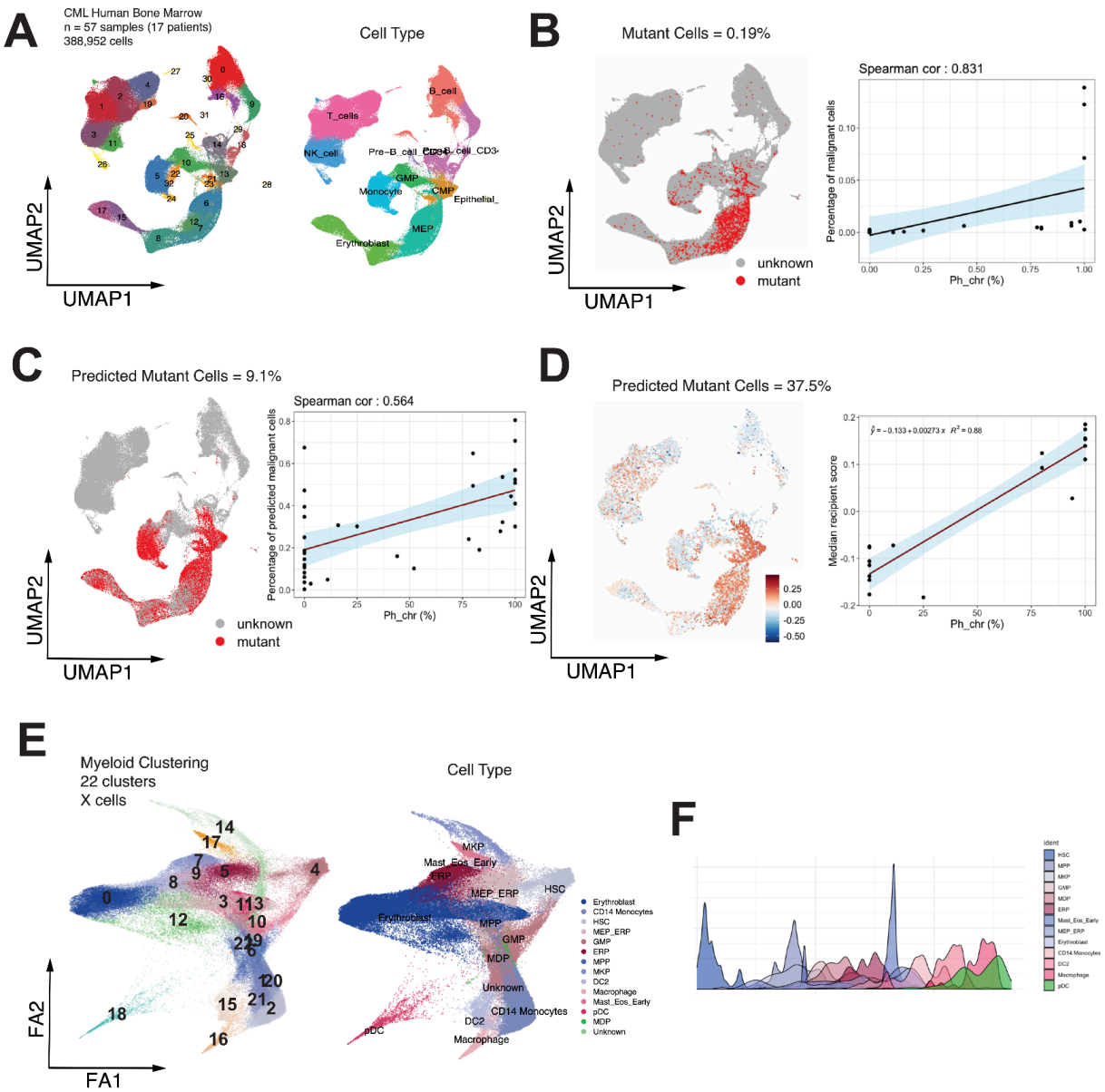
A
CML Human Bone Marrow
n = 57 samples (17 patients)
388,952 cells
Cell Type
UMAP2
UMAP1
T_cells
B_cell
NK_cell
Pre-B_cell_CD34-
B_cell_CD3-
GMP
Monocyte
CMP
Epithelial_
MEP
Erythroblast
B
Mutant Cells = 0.19%
unknown
mutant
Spearman cor : 0.831
Percentage of malignant cells
Ph_chr (%)
C
Predicted Mutant Cells = 9.1%
Spearman cor : 0.564
Percentage of predicted malignant cells
D
Predicted Mutant Cells = 37.5%
Median recipient score
E
Myeloid Clustering
22 clusters
X cells
FA2
FA1
MKP
Mast_Eos_Early
ERP
MEP_ERP
HSC
MPP
GMP
MDP
Unknown
CD14 Monocytes
DC2
Macrophage
pDC
F
ident

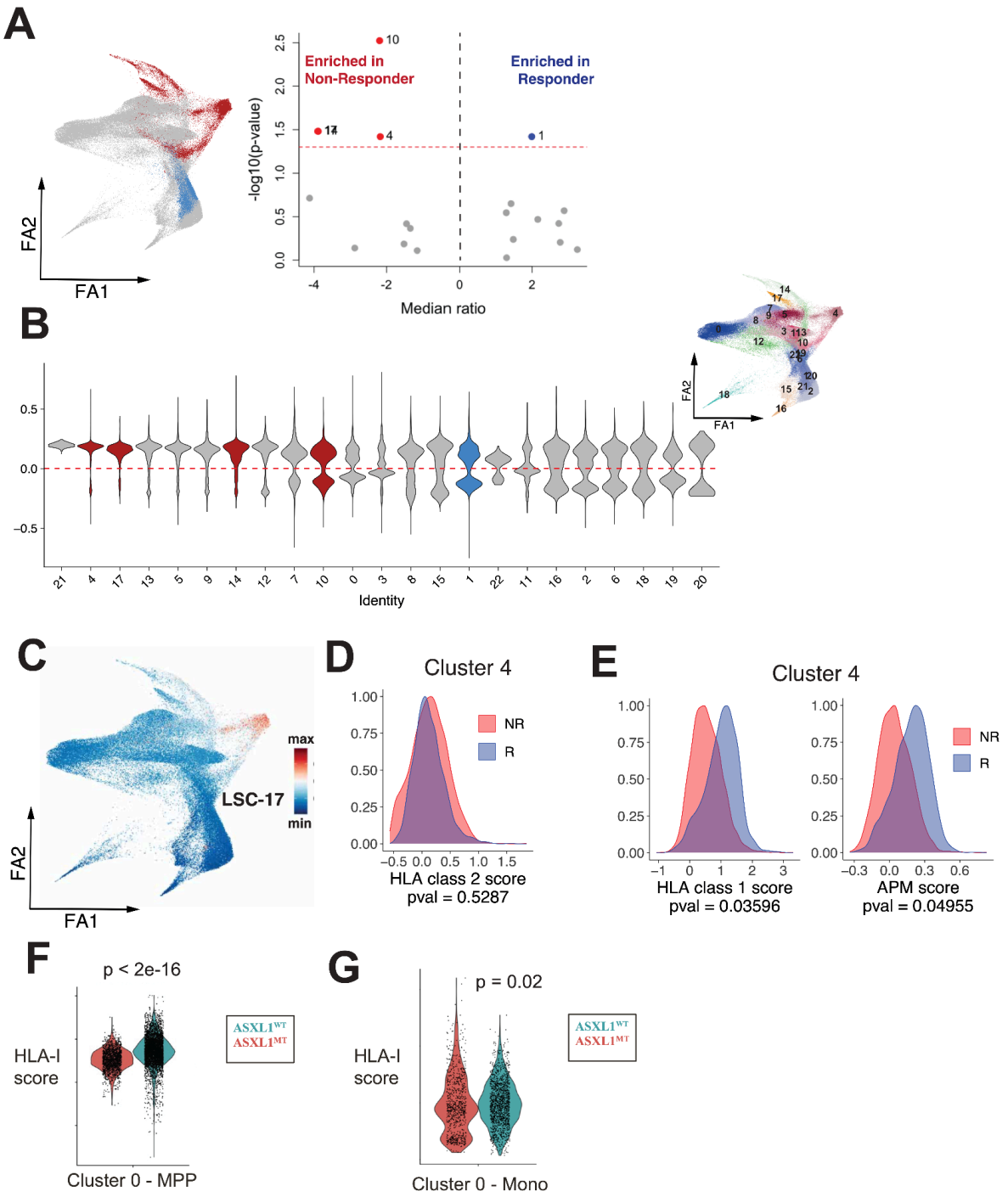
A
FA2
FA1
Enriched in Non-Responder
Enriched in Responder
-log10(p-value)
Median ratio
B
Identity
C
LSC-17
max
min
D
Cluster 4
NR
R
HLA class 2 score
pval = 0.5287
E
Cluster 4
HLA class 1 score
pval = 0.03596
APM score
pval = 0.04955
F
p < 2e-16
HLA-I score
Cluster 0 - MPP
ASXL1WT
ASXL1MT
G
p = 0.02
HLA-I score
Cluster 0 - Mono

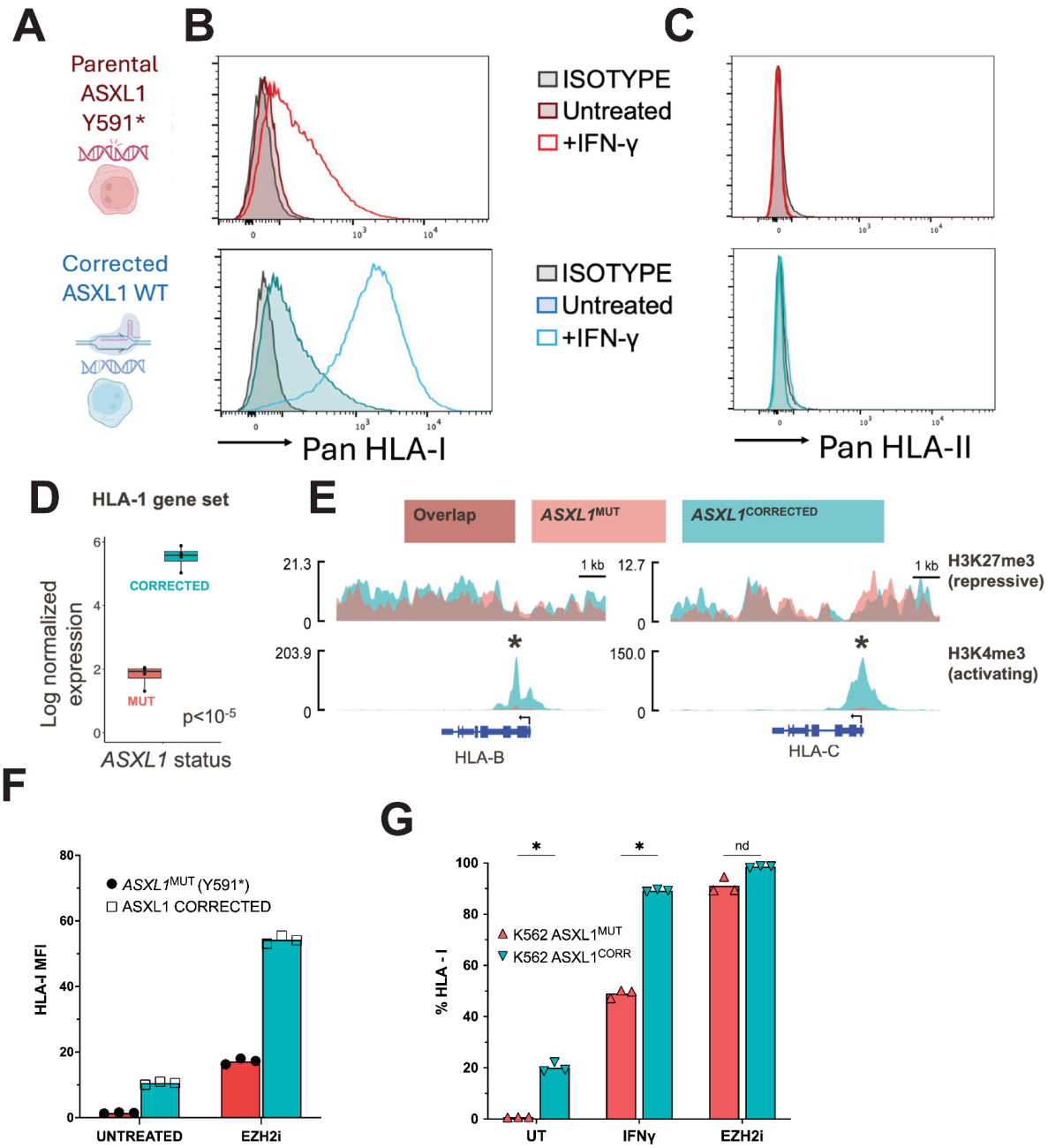
A
B
C
Parental
ASXL1
Y591*
Corrected
ASXL1 WT
ISOTYPE
Untreated
+IFN-γ
ISOTYPE
Untreated
+IFN-γ
Pan HLA-I
Pan HLA-II
D
HLA-1 gene set
Log normalized expression
CORRECTED
MUT
p<10-5
ASXL1 status
E
Overlap
ASXL1MUT
ASXL1CORRECTED
21.3
12.7
1 kb
H3K27me3 (repressive)
203.9
150.0
H3K4me3 (activating)
HLA-B
HLA-C
F
HLA-I MFI
ASXL1MUT (Y591*)
ASXL1 CORRECTED
UNTREATED
EZH2i
G
% HLA - I
K562 ASXL1MUT
K562 ASXL1CORR
nd
UT
IFNγ
EZH2i

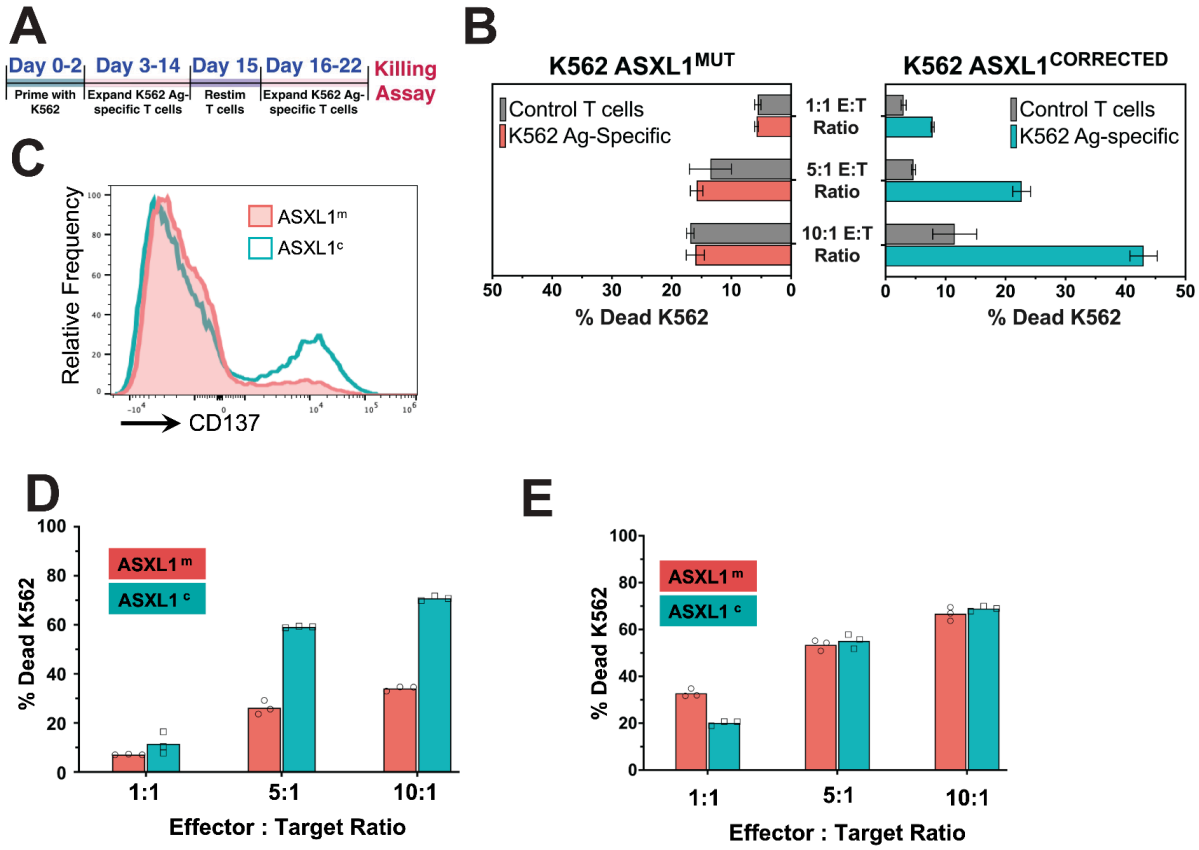
A
Day 0-2
Day 3-14
Day 15
Day 16-22
Killing Assay
Prime with K562
Expand K562 Ag-specific T cells
Restim T cells
Expand K562 Ag-specific T cells
B
K562 ASXL1MUT
K562 ASXL1CORRECTED
Control T cells
K562 Ag-Specific
Control T cells
K562 Ag-specific
1:1 E:T Ratio
5:1 E:T Ratio
10:1 E:T Ratio
% Dead K562
% Dead K562
C
Relative Frequency
ASXL1m
ASXL1c
CD137
D
% Dead K562
ASXL1 m
ASXL1 c
1:1
5:1
10:1
Effector : Target Ratio
E
% Dead K562
ASXL1 m
ASXL1 c
1:1
5:1
10:1
Effector : Target Ratio

Figure 1. Experimental design and identification of co-occuring mutations

(A) Clinical cohorts and external single-cell data sources analyzed.
(B) CoMut plot of detected mutations following Mutect2 with recipient-derived mesenchymal stromal cells (R-MSC) and donor peripheral blood cells (D-PBC) serving as normal controls.
(C) Lollipop plot of ASXL1 mutations identified the cohort. Insertions/deletions are identified as orange and nonsense mutations in red.
(D) Number of patients with exon 12 ASXL1 mutations in responders (n=9) and nonresponders (n=8) to DLI within the combined cohort. Significance calculated by Fishers Exact test.
(E) Increase in ASXL1 VAF at timpoints following DLI within patient 5318.
(F) TMB in reponders and nonresponders.

Figure 2. Identification of leukemic cells

(A) Single cell RNA-seq UMAP after harmonization and batch correction from BMMC of CML patients (n = 57 samples, 17 patients, 388,952 cells, 31 clusters) with cell type annotations.
(B) Predicted mutant cells after detection of mutations in single cell RNA-seq that were identified in whole exome sequencing.
(C) Predicted mutant cells after machine learning classification of mutant cells based upon identification of mutant cells by integration of single cell RNA-seq and whole exome sequencing.
(D) Identification of mutant cells by donor/recipient score assessed by transcripts arising from Y-chromosome.
(E) Single cell RNA-seq UMAP after harmonization and batch correction of myeloid cells composing 22 clusters.
(F) Cell states across pseudotime based upon Monocle 3 analysis.

Figure 3. Nomination of HLA-I suppression as a mechanism of resistance

(A) Clusters differentially enriched across patients in non-responders vs responders
(B) Clusters enriched in leukemic cells as assessed by donor/recipient score.
(C) LSC17 score nominates cluster 4 as a cluster composed of leukemic stem cells.
(D) HLA-II is not differentially enriched in responders or nonresponders within cluster 4.
(E) HLA-I and antigen-processing machinery (APM) score within cluster 4 identifies differential expression of these genes across responders and nonresponders..
(F) Suppressed HLA-I within leukemic stem cell clusters in an external scRNA-seq AML cohort.
(G) Reduced accessibility of HLA-I genes within leukemic stem cell clusters in an external scATAC-seq CMML cohort.

Figure 4. Experimental confirmation of epigenetic mediated suppression of HLA-I through ASXL1 mutations

(A) Experimental layout of K562 cell line generation
(B) HLA-I flow with and without IFNγ treatment

(C) HLA-II flow with and without IFNγ treatment
(D) RNA-expression of HLA-I genes in isogenic K562 cell lines
(E) SparK plots of H3K4me3 and H3K27me3 at HLA-B and HLA-C genes following CUT&RUN profiling
(F) Flow cytometry identification of HLA-I following 5 day treatment with EZH2i
(G) Flow cytometry identification of HLA-I following 9 day treatment with EZH2i and 24-hour treatment with IFNγ treatment

Figure 5. Correction of ASXL1 mutations or EZH2i pre-treatment restores T-cell attack
(A) Experimental layout of T cell generation
(B) Histogram demonstrating CD137 expression upon re-encounter with K562, either $K562^{m}$ or $K562^{c}$
(C) Comparison of K562 killing by control or K562 primed T cells
(D) Persistent differences in K562 killing following IFNγ pretreatment
(E) EZH2i pretreatment restores killing of $K562^{m}$